Lung Cancer 130 (2019) 25–34

Contents lists available at ScienceDirect

Lung Cancer

journal homepage: www.elsevier.com/locate/lungcan

PTEN inactivation induces epithelial-mesenchymal transition and metastasis by intranuclear translocation of β-catenin and snail/slug in non-small cell lung carcinoma cells

Perumal Elumalai[a,b,1], So Youn Kim[a,b,1], Sun Shin[a,b], Seung-Hyun Jung[a,b,d], Suji Min[a,b], Jieying Liu[a,b], Yeun-Jun Chung[a,b,c,*]

[a] Precision Medicine Research Center, Republic of Korea
[b] Integrated Research Center for Genome Polymorphism, Republic of Korea
[c] Department of Microbiology, Republic of Korea
[d] Cancer Evolution Research Center, The Catholic University of Korea, College of Medicine, Seoul, Republic of Korea

ARTICLE INFO

Keywords:
Lung cancer
PTEN
EMT
AKT/GSK-3β signaling
β-catenin

ABSTRACT

Objective: Epithelial-mesenchymal transition (EMT) is the key event in distant metastasis of diverse tumors including lung cancer. Recent evidence suggests the involvement of phosphatase and tensin homolog (PTEN) in EMT phenotypes. However, the molecular mechanism of EMT induced by PTEN inactivation is not clear in lung cancer. We aimed to investigate the role of PTEN inactivation in acquisition of EMT in lung cancer cells.
Methods: We knocked out the PTEN in PTEN proficient lung cancer cells lines (A549 and NCI-H460) using CRISPR/Cas-9 system and observed the growth, EMT phenotypes, and EMT related molecules. We also explored the in vivo effect of PTEN inactivation on tumor cell growth and distant metastasis using nude mouse injection.
Results: PTEN knockout (KO) cells showed faster growth, migration and invasion than PTEN wild-type (WT) cells. When we injected the cells into nude mice, PTEN-KO cells showed faster growth and higher metastatic potential. In PTEN-KO cells, the levels of phosphorylated AKT (Ser-473 and Thr-308) were profoundly elevated and the expressions of phosphorylated GSK-3β (Ser9, inactive form) increased, while that of β-catenin decreased. Regarding the EMT markers, the expression of E-cadherin decreased but those of N-cadherin, vimentin and MMP-2 increased in the PTEN-KO cells. Especially, PTEN-KO cells showed the almost complete intra-nuclear shift of β-catenin and no β-catenin signal was observed in the cell membrane. Accordingly, PTEN-KO cells exhibited morphological changes such as loss of cell-to-cell contact, pseudopodia and the round shape, which are the typical phenotypes of EMT. Snail and Slug were also dominantly accumulated in the nucleus after PTEN inactivation.
Conclusion: All these data consistently support that PTEN inactivation contributes to EMT by nuclear translocation of β-catenin and Snail/Slug in lung cancer cells.

1. Introduction

Lung cancer is the most common cancer worldwide and a leading cause of cancer related deaths with frequent recurrence and metastasis [1,2]. In spite of the recent remarkable development of new treatment strategies for lung cancer, such as tyrosine kinase inhibitors and immunotherapies, patient survival has not evidently improved. One of the key reasons of the high mortality is a high rate of metastasis, especially to brain and bone [3,4].

Epithelial-mesenchymal transition (EMT) is a process of morphological changes of epithelial cells in which polarized epithelial cells acquire mesenchymal phenotypes [5]. Through the EMT process, lung cancer cells lose cell-to-cell adhesion, acquire the ability to migrate, invade, and eventually metastasize [5,6]. Therefore, a better understanding of the molecular mechanism behind the EMT process in lung cancer is important for developing strategies to prevent metastasis and eventually decrease lung cancer mortality.

During oncogenesis, various genetic alterations are taken place

* Corresponding author at: Precision Medicine Research Center, College of Medicine, The Catholic University of Korea, 222 Banpo-daero, Socho-gu, Seoul, 06591, Republic of Korea.
E-mail address: yejun@catholic.ac.kr (C. Yeun-Jun).
[1] These two authors contributed equally to this work.

https://doi.org/10.1016/j.lungcan.2019.01.013
Received 10 August 2018; Received in revised form 26 December 2018; Accepted 27 January 2019

including activation of oncogenes and inactivation of tumor suppressor genes such as phosphatase and tensin homolog (*PTEN*) [7,8]. PTEN blocks PI3K-mediated AKT activation in the PI3K/AKT signaling pathway by dephosphorylating the phosphatidylinositol (3,4,5)-triphosphate (PIP3) [9]. PTEN plays a pivotal role in cell homeostasis by controlling cell cycle, apoptosis, adhesion, and migration [10]. Loss of PTEN expression occurs frequently in many types of cancers, which is reported to be involved in cancer progression and metastasis [11–13]. In non-small cell lung cancer (NSCLC), loss of PTEN expression has also been frequently (40~70%) observed [14–16].

Recent evidence suggests the involvement of PTEN in EMT. Kohnoh et al. reported that phosphorylation of PTEN C-terminus accelerates the EMT in lung cancer under hypoxic microenvironment [17]. Aoyama et al. suggested that transforming growth factor β (TGF-β) induces acquisition of malignant phenotypes such as EMT, which might be due to that TGF-β blocks normal PTEN activity through phosphorylation of PTEN C-terminus in lung cancer [18]. These data suggest that PTEN inactivation involves in acquisition of EMT phenotypes in lung cancer. However, the molecular mechanism of EMT induced by PTEN inactivation is not clear in lung cancer.

To investigate the role of PTEN inactivation in lung tumorigenesis, especially in acquisition of EMT, we knocked out the PTEN in PTEN proficient lung cancer cells using the CRISPR/Cas-9 system and observed the changes in EMT related molecules. We also explored the in vivo effect of PTEN inactivation on distant metastasis using nude mouse injection. Our data uncovered the novel roles of PTEN in lung cancer progression and metastasis.

2. Materials and methods

2.1. Antibodies

The following antibodies were purchased from Cell Signaling Technology (Danvers, MA, USA), against PTEN, Snail, Slug, phosphor-β-catenin, non-phosphor-β-catenin, AKT, phosphor- AKT^{s473}, phosphor-AKT^{t308}, phosphor-GSK-3β, phosphor-MEK, MEK, phosphor-ERK and Cyclin D1. Vimentin, N-Cadherin, E-cadherin, β-catenin, MMP-2, NFkP, SDF-1, CXCR-4, ERK and IL-8 were obtained from Santa Cruz Biotechnology (Santa Cruz, CA, USA). Anti-Lamin B1 was purchased from Abcam, (Cambridge, UK). Anti-β-actin was purchased from Sigma Aldrich (St. Louis, MO, USA). Anti-rabbit, anti-mouse and anti-goat secondary antibodies conjugated to HRP, FITC and TRITC were purchased from Santa Cruz Biotechnology.

2.2. Cell lines and culture

Non-small cell lung cancer cell lines (A549 and NCI-H460) were obtained from ATCC (Manassas, VA, USA) and grown in culture flasks containing RPMI 1640 medium supplemented with 10% FBS respectively, under 5% CO_2, 95% air at 37 °C. Upon reaching confluence, the cells were trypsinized and passaged.

2.3. Generation of stable PTEN knockout cell lines by CRISPR/Cas9 system

To generate the PTEN knockout (KO) cell line, we used a genome-editing tool, CRISPR/Cas9 system. A PTEN CRISPR/Cas9 KO plasmid (Santa Cruz, sc-400103) contains a pool of three plasmids, a target-specific 20 nt guide RNA designed to delete the PTEN by the double-strand break within the gene, Cas9 nuclease and green florescence protein (GFP) coding sequences for visualization of transfection. A PTEN homology-directed DNA repair (HDR) plasmid (Santa Cruz, sc-400103-HDR) encodes a homology-directed DNA repair template for the double-strand break, which incorporates the puromycin resistance gene for selection of PTEN KO cells and red florescence protein (RFP) to visually confirm transfection. A control CRISPR/Cas9 plasmid (sc-418922) containing 20 nt non-targeting gRNA and GFP was designed for a negative control. A 60 mm dish was plated with 2×10^5 cells and the cells were transfected after obtaining 60% confluence. The PTEN CRISPR/Cas9 KO plasmid (1.5 μg) and the PTEN HDR plasmid (1.5 μg) were mixed with 4 μl of lipofectamine 2000 reagents (Invitrogen, Eugene, OR, USA) and co-transfected into A549 and NCI-H460 cells. After 48 h transfection, 0.5 μg of puromycin was added for 7–10 days to select positively transfected cells. After puromycin selection, stable PTEN-KO single colonies were isolated and expanded separately. After expansion, cell lysates were collected to assess the PTEN expression.

2.4. Cell proliferation assay and growth rate determination

Proliferation rates of PTEN-KO and PTEN-WT cell lines were assessed by cell counting kit-8 (Dojindo Laboratories, Kumamoto, Japan). A volume of 250 μl of cell suspension (1.0×10^4) were plated in 48-well plates and incubated for 24 h and 48 h. After incubation, 20 μl of CCK-8 solution was added to the plates, which were incubated for 2 h in the CO_2 incubator. The absorbance at 450 nm was measured using a microplate reader. To determine the growth rate, 1.0×10^5 cells were seeded in 6-well plates, incubated and counted at 24 h, 48 h and 72 h.

2.5. Western blot analysis

The cells were cultured in 100 mm dishes and washed with 1X PBS after incubation and lysed with RIPA buffer containing protease inhibitors. Protein concentrations were estimated using Bradford protein assay (BioRad, Hercules, CA, USA). A volume of 30–50 μg of protein lysates were electrophoresed on 10–12% SDS polyacrylamide gels and then transferred onto PVDF membranes. The membrane were incubated with 5% nonfat dry milk/1X TBS to block non-specific binding followed by incubation with primary antibodies (diluted according to the manufacturer's instruction). After primary antibody incubation, the membranes were washed with 1X TBST, followed by incubation with HRP conjugated anti-mouse IgG or anti-rabbit IgG secondary antibodies. Protein bands were visualized using a super signal west pico chemiluminescence system (Thermo Scientific, Rockford, IL, USA).

2.6. Quantitative real-time PCR

Total RNA was isolated by using Tri Reagent (Sigma Aldrich, St. Louis, MO, USA). Two μg of total RNA from each sample was reverse-transcribed using the Superscript III first strand cDNA synthesis kit (Invitrogen, CA, USA). RT-PCRs were performed using the primers targeting chemokines (**Table. S1**). RT-PCR was carried out in an applied biosystems machine (Applied Biosystems Inc, CA, USA). Reaction was performed using the Ampone taq premix PCR master mix, which contains all PCR components along with SYBR green dye (Geneall Biotechnology, Seoul, South Korea). The specificity of the amplification product was determined by melting curve analysis for each primer pair. Data were analyzed by comparative C_T method and the fold change is calculated by $2_T^{-\Delta\Delta C}$ method described by Schmittgen and Livak [19].

2.7. Migration and invasion assay

Transwell migration assay was performed to assess the migration potential of PTEN-KO cells. Matrigel inserts (Corning, NY, USA) were rehydrated with serum-free RPMI-1640 for 2 h. Cells were harvested and 1×10^5 cells were suspended in 0.2 ml of serum-free medium. They were added to the upper chamber of transwell inserts and 0.5 ml of 10% FBS medium was added in the lower chamber. After 16 h and 32 h incubation, non-migrated cells in the upper chamber were removed and migrated cells in the lower chamber were fixed with ethanol and stained with 0.5% crystal violet. The migrated cells were captured by phase contrast microscope in ×100 magnification and counted randomly from five fields. The invasion assay was performed using the Corning Biocoat Matrigel invasion chamber (Corning) in the same way

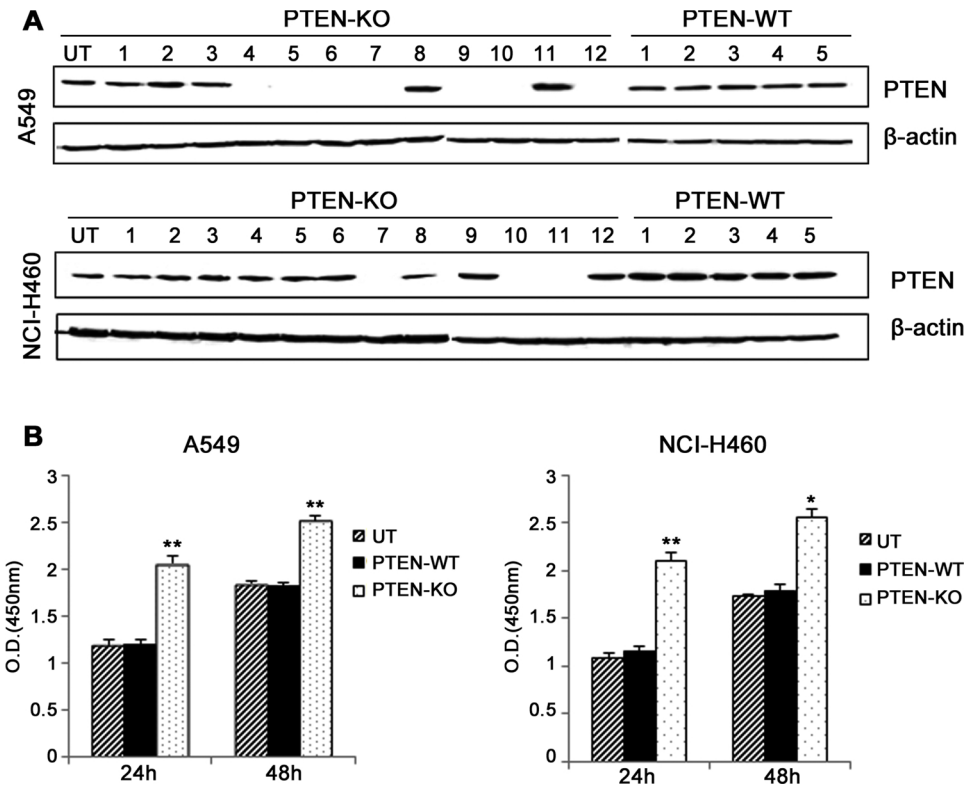

Fig. 1. Construction of PTEN-knockout lung cancer cell lines by CRISPR/Cas9.
(A) PTEN expression in untreated control (UT), PTEN wild-type stable clones treated with CRISPR/cas9 control plasmid (PTEN-WT) and PTEN-knockout (PTEN-KO) stable clones. Ten PTEN-KO clones showed complete loss of PTEN expression. (B) The effect of PTEN deficiency on proliferation. Clone 7 for A549 and Clone 11 for NCI-H460 were analyzed by CCK-8 at the indicated times. Proliferation of both lung cancer cell lines with silenced PTEN increased compared with PTEN-WT and -UT cells (in A549 at 24 h: 1.20 ± 0.047 in UT, 1.19 ± 0.05 in WT vs. 2.06 ± 0.08 in KO; in A549 at 48 h: 1.84 ± 0.033 in UT, 1.82 ± 0.035 in WT vs. 2.52 ± 0.055 in KO). (in NCI-H460 at 24 h: 1.07 ± 0.06 in UT, 1.14 ± 0.05 in WT vs. 2.10 ± 0.07 in KO; in NCI-H460 at 48 h: 1.73 ± 0.017 in UT, 1.78 ± 0.060 in WT vs. 2.55 ± 0.08 in KO). Data are presented as mean ± SEM from three independent experiments. $*P < 0.05$; $**P < 0.01$ vs. PTEN-WT.

as the migration assay except that Matrigel was coated above the membrane in the invasion assay.

2.8. Scratch wound healing assay

A549 and NCI-H460 cells (2×10^5 cells/well) were plated in 6-well culture plates in RPMI-1640 containing 10% FBS. After 24 h, the cell monolayer was scraped with a sterile 200 µl micropipette tip to create a wound, and photographed using inverted microscope at 0 h, 16 h and 32 h. The relative migration distance was measured by image J software and calculated by the following formula: relative migration distance (%) = 100 (A–B)/A, where A is the width of cell wounds before incubation, and B is the width of cell wounds after incubation. All experiments were carried out in triplicate.

2.9. Colony formation assay

The cells were trypsinized and 1000 cells were plated for colony formation assay in 100 mm petri dishes and cultured for 10 days. Finally, the plates were washed with PBS, fixed in methanol for 20 min and then stained with 0.4% crystal violet for 30 min at room temperature. The plates were distained and photographed. All experiments were carried out in triplicate.

2.10. Immunocytochemistry

A549 and NCI-H460 cells were cultured in chambered slides (SPL Life Sciences, Gyeonggi-do, South Korea). After 24 h incubation, the cells were fixed in 4% paraformaldehyde for 15 min, followed by washing with PBS, and then incubated for 15 min in 0.5% Triton X-100 in PBS. The cells were blocked with 5% BSA for 1 h at room temperature, washed and incubated with primary antibodies for overnight at 4 °C. After washing three times with PBS, the cells were incubated with secondary antibodies conjugated with FITC/TRITC for 1 h and stained with nuclear stain Hoechst 33342 for 10 min and mounted. The cells were photographed using confocal microscope (LSM 510 Meta, Zeiss, Oberkochen, Germany).

2.11. In vivo tumorigenesis and metastasis Model

BALB/c-nu female mice (6 weeks old) were purchased from Jackson Laboratory (Sacramento, CA, USA), maintained and treated under specific pathogen-free conditions. PTEN-WT and PTEN-KO A549 cells (1×10^6 cells/mouse) were injected subcutaneously (six mice per group). Tumor growth rates were monitored by measuring tumor diameters twice per week and tumor growth curves were recorded accordingly. After 4 weeks, mice were sacrificed and tumors were weighed. To produce distant metastasis, 1×10^6 cells were injected via the tail vein of 6 week-old BALB/c-nu female mice (12 mice per group). After seven weeks, mice were sacrificed and organs (lung, heart, liver, spleen, kidney, brain, and inguinal LN) were collected and evaluated by hematoxylin and eosin staining. When a metastatic focus was observed in any of the organs, the mouse was counted as distant metastasis positive. All animal experimental procedures were approved by The Catholic University of Korea Animal Ethics Committee (CUMS-2016-0251-03).

2.12. Statistical analysis

All experiments were repeated at least two times. For all measurements, One-way ANOVA followed by Students Newman-Keul's (SNK) test was used to assess the statistical significance of differences between PTEN-WT and PTEN-KO cells. A P value of < 0.05 was considered statistically significant.

3. Results

3.1. Increased cell proliferation in PTEN-KO lung cancer cell lines

To investigate the tumorigenic implication of PTEN loss in lung cancer cells, we knocked out the *PTEN* gene in PTEN proficient NSCLC cells (A549 and NCI-H460) using the CRISPR/Cas-9 system. The PTEN

CRISPR/Cas9 KO plasmid (herein after called PTEN-KO-plasmid) and the PTEN HDR plasmid are co-transfected into the A549 and NCI-H460 cells. The PTEN-KO plasmid was designed to modify the *PTEN* gene sequence, which introduces a premature stop codon and eventually stop the expression of functional protein by inducing double-strand break in a 5′ constitutive exon of *PTEN* gene where GFP gene was incorporated to visually confirm the transfection. The PTEN-HDR-plasmid contains the RFP gene for confirming transfection and the puromycin resistance gene for selection of stable cells containing successful double-strand break. After puromycin selection, each colony was expanded separately and the clones with the complete loss of PTEN were confirmed by western blotting (Fig. 1A). Seven clones from A549 and three clones from NCI-H460 cells showed the complete loss of PTEN expression. To explore the biological consequences of inactivating PTEN, we selected two PTEN-KO clones (clone 7 for A549 and clone 11 for NCI-H460) for all following experiments. As a control, empty plasmid transfected cells (PTEN-WT) were used. We checked the cell proliferation and growth rates of both PTEN-KO and PTEN-WT cells. PTEN-KO cells showed the significantly increased proliferation compared with PTEN-WT cells in both A549 and NCI-H460 cells (Fig. 1**B and Fig. S1**). Both PTEN-WT cells and plasmid-construct untreated cells showed almost identical proliferation rates, suggesting that the cytotoxic effect of plasmid transfection was negligible for both cells.

3.2. Increased cell migration and invasion in PTEN-KO lung cancer cell lines

We next explored the effects of PTEN-KO on migration and invasion of lung cancer cells. For this, we performed the scratch wound healing assay and the matrigel transwell assay. After obtaining 80% confluence, the cell monolayer was scratched using a 200 µl tip (defined as 0 h). Wound closure of PTEN-KO cells was significantly faster than that of PTEN-WT cells at both 16 h and 32 h after scratching (Fig. 2A). In the transwell migration assay, cohering with the wound healing assay, PTEN-KO cells showed a significantly higher number of migrated cells compared with PTEN-WT cells (Fig. 2B). We also compared the invasiveness of PTEN-KO and PTEN-WT cells using the transwell invasion assay. The number of cells that passed through the extracellular matrix coated insert plate was significantly higher in PTEN-KO cells than in PTEN-WT cells in both cells (Fig. 2C). PTEN-WT and untreated cells showed almost identical ranges of migration and invasion, supporting that plasmid transfection did not affect these phenotypes.

3.3. Effect of PTEN-KO on tumorigenicity and metastasis in nude mice

To explore the in vivo effect of PTEN-KO, we observed the tumorigenicity and metastasis of the PTEN-KO A549 cells in nude mice. First, PTEN-KO and PTEN-WT cells were subcutaneously injected and the tumor size was monitored for 28 days. After subcutaneous injection, the growth of the PTEN-KO cells was significantly faster than that of the PTEN-WT cells in nude mice **(**Fig. 3**A and B).** Second, the metastatic potential of the PTEN-KO cells was evaluated in nude mice by tail vein injection. Seven weeks after tail vein injection, 67% (8/12 mice) were positive for metastasis in the PTEN-KO cell injected mice and 4 of them (50%) showed multi-organ metastases, whereas 25% (3/12) were positive in the PTEN-WT cell injected mice and none of them showed multi-organ metastases. Examples of organ metastasis in the PTEN-KO and PTEN-WT cell injected mice are available in **Fig. S2**.

3.4. AKT signaling pathway activated by PTEN loss in lung cancer cells

To explore the mechanisms of increased tumor growth and metastasis in PTEN-KO cells, we first examined the expression or activities of the PI3K/AKT/GSK-3β pathway. Levels of total AKT expression were not different between PTEN-KO and PTEN-WT cells. However, the levels of phosphorylated AKT (p AKT) at both Ser-473 and Thr-308 were profoundly elevated in PTEN-KO cells compared with PTEN-WT cells (Fig. 4A). When we observed the downstream protein targets, expression of phosphorylated GSK-3β (pGSK-3β) (Ser9) (inactive form), phosphorylated β-catenin (inactive form), NFkB p65 and cyclin D1 increased, while that of β-catenin decreased in the PTEN-KO cells. The expression of non-phosphorylated (active form) β-catenin (Ser33/37/Thr41) protein, which is the main player of cell-to-cell adhesion, also decreased in PTEN-KO cells (Fig. 4A). To explore whether the activation of AKT in PTEN-KO cells facilitated the nuclear translocation of β-catenin, we performed the immunocytochemistry analysis targeting β-catenin. PTEN-KO cells showed the almost complete intra-nuclear shift of β-catenin and no β-catenin signal was observed in the cell membrane in both cells. Contrary to this, a majority of β-catenin is located in the cell membrane and just trace amounts are in the nucleus of PTEN-WT cells (Fig. 4B). When we checked the mutation status of the *PI3K* gene, the results were consistent with previously known data: no mutation in A549 cells and a mutation in NCI-H460 (Exon-9, p.E545 K) (data not shown).

3.5. Alteration of EMT markers and induction of metastasis related chemokine expression through activation of AKT by PTEN-KO

Activation of AKT in PTEN-KO cells suggests that loss of PTEN may affect the EMT pathway, which can facilitate the tumor metastasis. To explore this possibility, we examined the expressions of the EMT markers. As expected, the expression of E-cadherin expression decreased in PTEN-KO cells, but the expressions of N-cadherin, vimentin and MMP-2 increased compared with PTEN-WT cells in both lung cancer cells (Fig. 4C). When we examined the signal intensity and intracellular localization of the EMT markers by immunocytochemistry, membrane localization of E-cadherin, an epithelial marker protein, was almost completely lost in PTEN-KO cells, but prominent in PTEN-WT cells in both lung cancer cells (Fig. 4D). In contrast, the signals of mesenchymal markers, N-cadherin and vimentin, increased in PTEN-KO cells compared with the PTEN-WT cells (Fig. 4**E and F**). When we quantify the fluorescence signal intensities of immunocytochemistry images of EMT related proteins, those are compatible with western blot data (**Fig. S3**). Interestingly, PTEN-KO cells exhibited morphological changes such as loss of cell-to-cell contact, pseudopodia and the round shape, which suggest EMT (Fig. 4G). In the colony formation assay, the colony shape of PTEN-KO cells became fuzzy in both cells (Fig. 4G**).** When we examined other regulators of EMT in PTEN-KO cells, expressions of Snail, Slug and MMP-2 increased compared with PTEN-WT cells (Fig. 4C). Chemokines are also known to play an important role in the regulation of EMT and metastasis. To further explore the potential implication of PTEN on the expression of metastasis-related chemokines, we observed the expressions of chemokines (CXCL8 and CXCL12), and chemokine receptors (CXCR1 and CXCR4). The protein expressions of CXCL8, CXCL12 and CXCR4 profoundly increased in PTEN-KO cells (Fig. 4C). RNA expression levels of these chemokines were consistently elevated (**Fig. S4**). Expression of CXCR1 was not detectable by western blotting, but its mRNA level increased significantly (**Fig. S4**).

3.6. Upstream mechanism of AKT activation in PTEN-KO cells

To understand the mechanism of AKT activation in PTEN-KO cells, we explored the role of PI3K, an upstream molecule of the AKT/GSK-3β pathway. We examined whether there is a reversal effect of AKT activation in PTEN-KO cells after blocking PI3K. After treating PTEN-KO cells with the PI3K inhibitor (LY294002), pAKT (Ser-473 and Thr-308), pGSK-3β, p-β-catenin and cyclin D1 levels were downregulated in both cell lines, similar to the effect on PTEN-WT cells (Fig. 5**A and Fig. S5**). However, the levels of PTEN, β-catenin, non-p-β-catenin, and NFKB p65 did not change significantly after the treatment (**Fig. S5**). To understand the downstream mechanism of PTEN loss mediated EMT activation, we also explored the reversal effect of LY294002 treatment on the

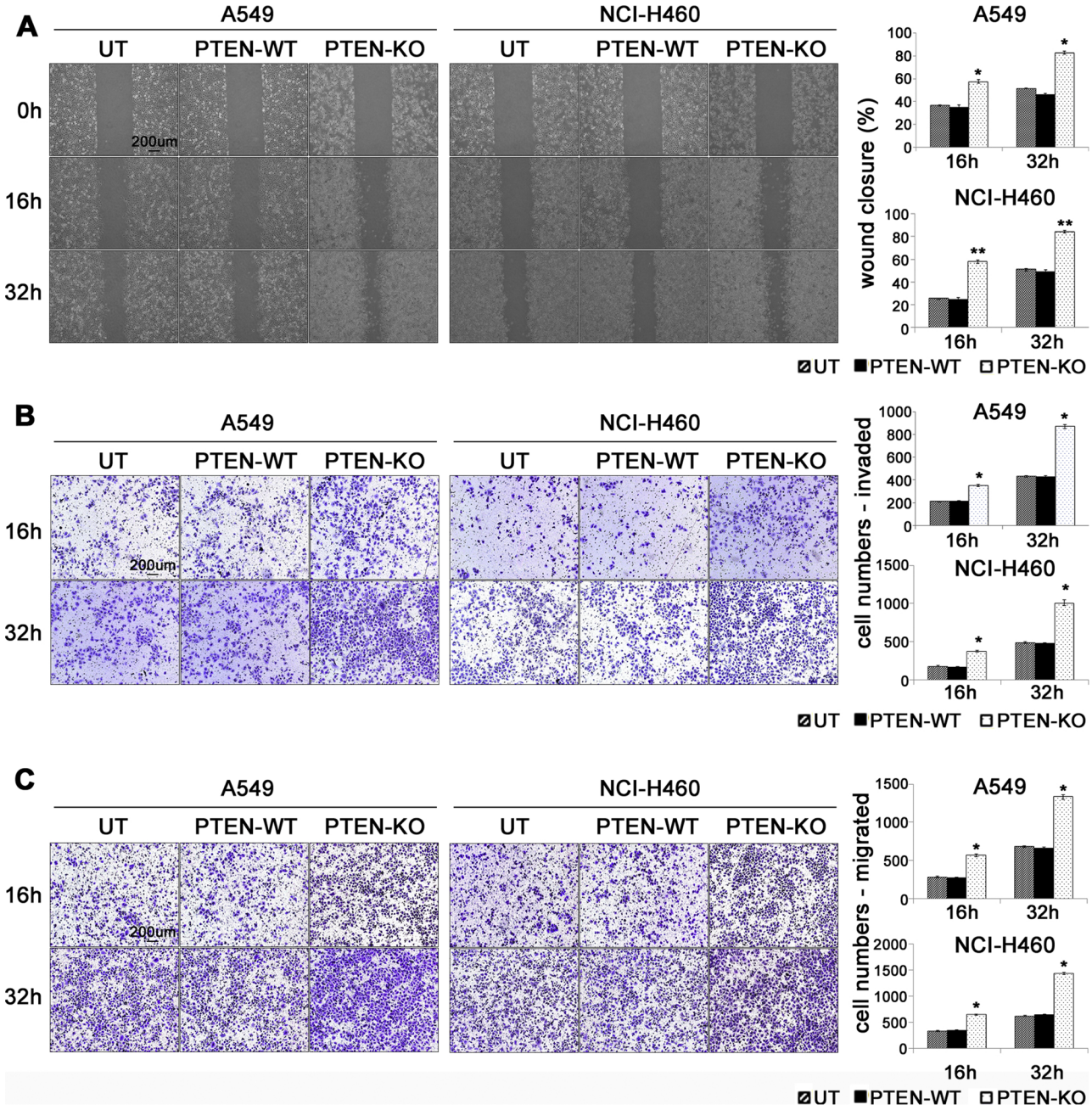

Fig. 2. Wound healing, migration and invasion of A549 and NCI-H460 stimulated by PTEN deficiency. (A) Wound healing assay in untreated control (UT), PTEN-WT and PTEN-KO lung cancer cells in vitro. Images show wound closures monitored by scratch wound healing assay done on PTEN-deficient A549 and NCI-H460 cells. Graphs show the quantification of relative wound closure manipulated with Image J program. Wound closure percentage in PTEN-KO cells was markedly higher (in A549 at 16 h: 36.64 ± 0.27% in UT, 35.18 ± 1.85% in WT vs 57.54 ± 54% in KO; in A549 at 32 h: 51.6 ± 0.34% in UT, 46.07 ± 1.01% in WT vs 82.96 ± 1.29% in KO). (in NCI-H460 at 16 h: 25.12 ± 0.76% in UT, 24.71 ± 1.44% in WT vs 57.80 ± 1.44% in KO; in NCI-H460 at 32 h: 50.54 ± 1.09% in UT, 49.17 ± 1.60% in WT vs 83.98 ± 1.11% in KO). (B&C) Effects of PTEN on invasion and migration of lung cancer cells in vitro. Cells were counted in five random fields at x100 magnification after 16 h and 32 h incubation. (B) Invaded cell numbers: in A549 at 16 h: 209.3 ± 6.03 in UT, 214 ± 5.8 in WT vs. KO 351.0 ± 8.31 in KO; in A549 at 32 h: 431 ± 7.89 in UT, 429.3 ± 8.0 in WT vs. 869.3 ± 15.43 in KO. in H460 at 16 h: 179.3 ± 6.8 in UT, 168.3.0 ± 6.66 in WT vs. 374.3 ± 12.92 in KO; in H460 at 32 h: 488.3 ± 13.88 in UT, 474.3 ± 12.68 in WT vs. 1010.6 ± 40.53 in KO. (C) Migrated cell numbers: in A549 at 16 h: 280.3 ± 10.13 in UT, 272.3 ± 8.61 in WT vs. 565 ± 19.09 in KO; in A549 at 32 h: 680.3 ± 9.47 in UT, 661 ± 12.22 in WT vs. 1333 ± 29.94 in KO. in H460 at 16 h: 330.6 ± 9.89 in UT, 341 ± 9.26 in WT vs. 645 ± 13.63 in KO; in H460 at 32 h: 616.6 ± 11.78 in UT, 642.3 ± 9.53 in WT vs. 1434 ± 23.55 in KO. Data are presented as mean ± SEM from three independent experiments. *$P < 0.05$; **$P < 0.01$ vs. PTEN-WT.

nuclear translocation of β-catenin, Snail and Slug, and membrane localization of E-cadherin. In untreated PTEN-KO cells, β-catenin expression disappeared in the cellular membrane and was accumulated in the nucleus. Contrary to this, in treated PTEN-KO cells, a substantial amount of β-catenin remained in the cell membrane (Fig. 5**B** and **Fig. S6A**). Regarding Snail and Slug, in terms of subcellular localization, both molecules were dominantly accumulated in the nucleus in untreated PTEN-KO cells. However, in LY294002 treated PTEN-KO cells, nuclear translocation of these molecules become profoundly reduced (Fig. 5**C** and **D**). Regarding E-cadherin, there was no reversal effect on the membrane localization (**Fig. S6B**). When we observed the protein expression level of EMT related proteins, Snail, Slug, CXCL8 and

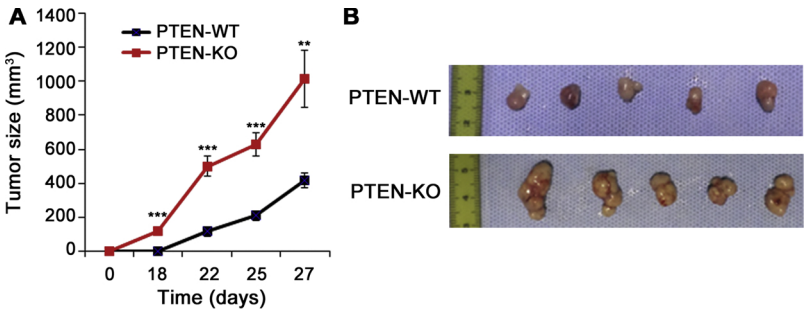

Fig. 3. High tumorigenic potential of PTEN-KO cells in nude mice xenograft model. To establish a xenografts model, six-week old BALB/c nu mice were injected subcutaneously with (1×10^6 cells/mouse, six mice for each group) PTEN-WT and PTEN-KO A549 cells. Tumor volumes were measured twice per week for 28 days post-injection. Finally, five mice were measured per each group, because two of them died during the observation. (A) Significant changes in tumor volume measured and blotted in the graph (Day 18, WT 0 mm^3 vs KO 117.3 ± 17.5mm^3; Day 22, WT 117.5 ± 27.3mm^3 vs. KO 500.4 ± 57.1mm^3; Day 25, WT 210.3 ± 25.9mm^3 vs. KO 625.7 ± 67.9mm^3; Day 27, WT 416.7 ± 41.2mm^3 vs. KO 1012.7 ± 169.4mm^3). $^{**}P < 0.01$; $^{***}P < 0.001$ vs. PTEN-WT. (B) Xenograft tumors in PTEN-KO and PTEN-WT groups.

CXCL12 were downregulated, while those of E-cadherin, N-cadherin, vimentin, MMP-2 and CXCR4 did not change significantly after LY294002 treatment in both WT and KO cells (**Fig. S7**). Subsequently, we examined the MAPK pathway proteins, MEK and ERK. PTEN inactivation triggered the phosphorylation of MEK and ERK in both PTEN-KO cells (**Fig. S8A**). LY294002 treatment moderately decreased the phosphorylation of ERK in PTEN-KO cells, but did not change those of pMEK, MEK and ERK in both WT and KO cells (**Fig. S8B**).

4. Discussion

EMT is the key event in distant metastasis, in which epithelial cells lose their marker proteins and acquire the mesenchymal marker proteins [20]. PTEN plays a pivotal role in cell homeostasis through negative regulation of PI3K mediated AKT activation. Loss of PTEN has been commonly observed in lung cancer and inactivation of PTEN has been suggested to be involved in acquisition of EMT phenotypes in lung cancer [17,18]. However, detailed mechanisms behind AKT activation in PTEN inactivated lung cancer cells are not clear. Regarding the inactivation of PTEN, a number of studies have reported that substantial proportion of lung cancers had complete loss of PTEN expression. For example, Yanagawa et al. reported that complete loss of PTEN expression was observed in 41.4% of NSCLCs [21]. In Soria et al.'s study, 24% of NSCLCs were PTEN expression negative. When they observed 16 NSCLC cell lines, five of them displayed weak PTEN expression and another five had no PTEN expression [14]. These data suggest that, complete loss of PTEN is not uncommon in NSCLC. Therefore, in this study, we explored the molecular mechanism behind the effects of complete inactivation of PTEN on EMT in lung cancer by knocking out *PTEN* gene in PTEN proficient NSCLC cells using the CRISPR/Cas-9 system. We uncovered the novel roles of PTEN in EMT and metastasis of NSCLC as follows (Fig. 6): When inactivated, PTEN loses its negative regulatory role in PI3K-mediated AKT activation. Activated AKT (pAKT) impedes GSK-3β activity by ser9 phosphorylation, which results in β-catenin stabilization in cytosol and subsequent nuclear translocation. pAKT also induces nuclear translocation of EMT-related molecules such as Snail and Slug [22–24]. Translocated β-catenin increases the transcription of cyclin D1 and EMT target genes in the nucleus, and the elevation of Snail/Slug in the nucleus represses the transcription of E-cadherin, which consequently inhibits the cell-to-cell adhesion and accelerates migration, invasion and metastasis of lung cancer cells. In addition, β-catenin localization in the membrane decreased in PTEN-KO cells, which is involved in cell-cell interaction along with E-cadherin.

To mimic PTEN inactivation in PTEN proficient primary NSCLCs, we developed stable PTEN-KO NSCLC cell lines. Although there have been several PTEN knockdown studies, the knockdown effects were incomplete and transient, and none identified the AKT/β-Catenin/Snail pathway in lung cancer [25,26]. This is the first study that induced complete inactivation of PTEN by CRISPR/Cas9 in lung cancer cells. PTEN deficient NSCLC cells showed a significantly increased proliferation rate, faster wound closure and migration/invasion phenotypes. All these data support that PTEN inactivation can contribute to the metastatic potential of NSCLC. Our data is consistent with the previous observations in diverse cancers including lung cancer [13,27]. These in vitro characteristics were recapitulated in a xenograft nude mouse model. Cho et al. reported that silencing of PTEN increases melanoma incidence in mice bearing tumors but not significantly promote distant metastasis [28]. In our study, tumor growth was significantly faster in PTEN-KO cells than in PTEN-WT cells. We did not observe the in vivo growth of plasmid-construct untreated cells because in vitro results consistently suggested that the cytotoxic effect of plasmid transfection was negligible. Also, after tail vein injection, distant metastasis masses were more frequently observed in PTEN deficient lung cancer cells. Interestingly, PTEN deficient cells showed loss of cell-cell contact, pseudopodia and the round shape, which are the typical EMT phenotypes. Previously, Rho et al. reported that gefitinib-resistant lung cancer cells acquired EMT phenotypic changes such as pseudopodia formation and spindle shape cells with increased mesenchymal proteins and decreased epithelial marker proteins [29]. All these data support that PTEN inactivation may be involved in metastasis of NSCLS through aggravating EMT.

Next, we explored the molecular mechanism of EMT phenotypic changes. The PI3K/AKT/GSK-3β pathway is the key component of the EMT signaling pathway and known to induce cancer cell migration and invasion [28,30]. In our study, the pAKT level increased profoundly and the expression of pGSK-3β (Ser9), an inactive form, also increased. pAKT is known to impede GSK-3β activity by ser9 phosphorylation, which results in β-catenin stabilization in cytosol and facilitates nuclear translocation of β-catenin [31]. Nuclear accumulation of β-catenin activates LEF/Tcf transcription factors, which promote the expression of EMT-related genes [32]. In this study, we observed that the protein expression of β-catenin targets, cyclin D1 and NFkB, increased in PTEN-KO cells. Previous studies also reported that AKT-mediated phosphorylation of β-catenin induces its nuclear translocation and enhances its transcriptional activity, which leads to tumor progression [22]. Snail, Slug and MMP-2 play important roles in regulation of EMT, by suppressing E-cadherin expression [33]. We found that PTEN-KO cells showed increased Snail and Slug expression which may inhibit E-cadherin and β-catenin interaction in the membrane and release β-catenin from the membrane. Loss of membrane localization of β-catenin leads to loss of cell-cell interaction and promote cell migration and invasion in PTEN-KO cells. Interestingly, total protein expression of β-catenin decreased in PTEN-KO cells. It may be due to loss of β-catenin substrate protein E-cadherin and/or proteosomal degradation of β-catenin caused by Akt-mediated phosphorylation. We observed that protein expression of phosphorylated β-catenin significantly increased in PTEN KO cells. A similar study also reported that Hes1-meditated PTEN inhibition causes reduced expression of membrane and cytoplasmic β-catenin, but not nuclear accumulation in NPC cells [30]. In our study, β-catenin clearly decreased in the membrane and translocated into the nucleus, which may induce EMT in PTEN-KO cells.

Chemokines play important roles in leukocyte cell trafficking and metastasis of cancer cells. CXCL8 is a pro-inflammatory CXC chemokine

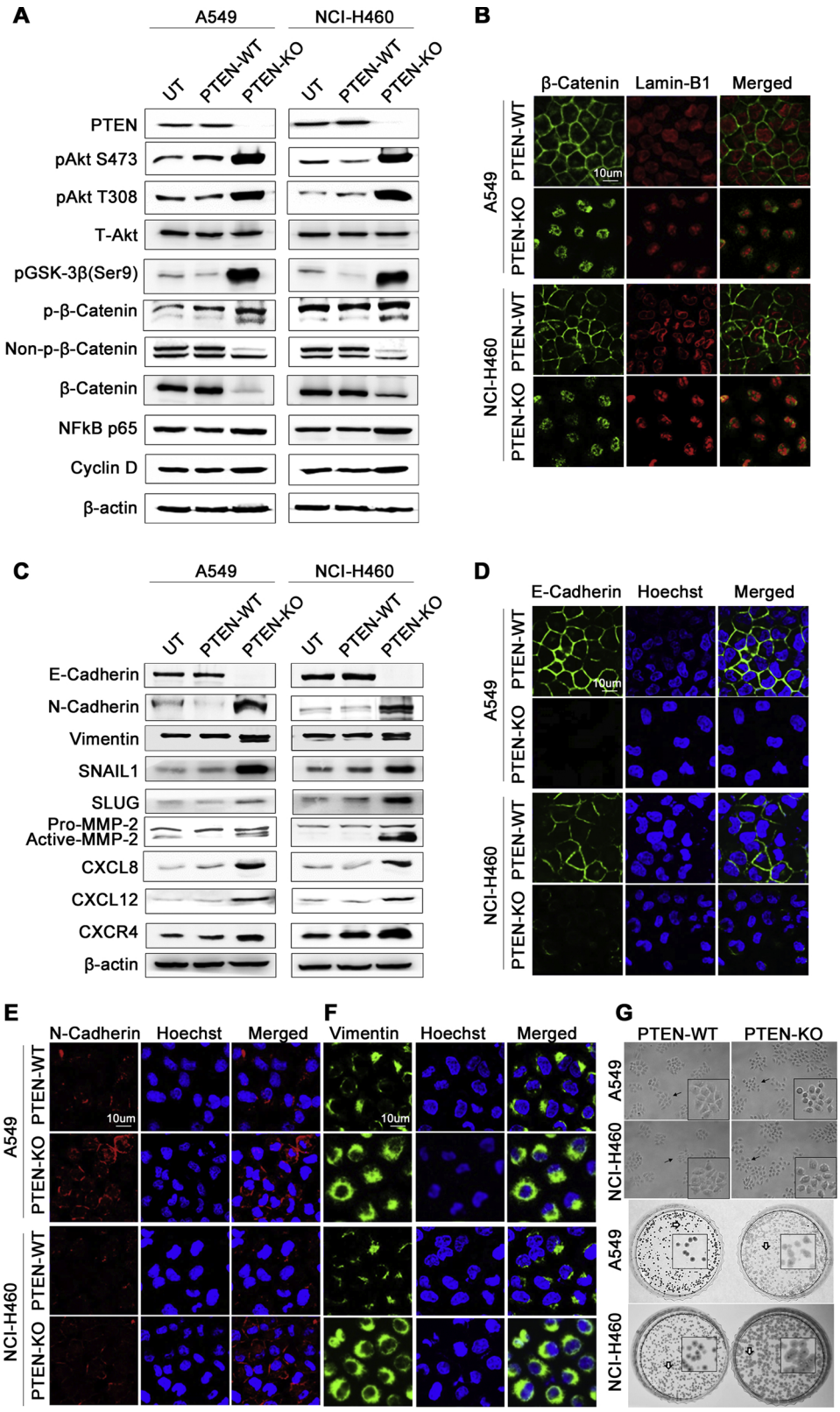

Fig. 4. Protein expressions of PTEN signaling molecules and EMT markers in PTEN-KO lung cancer cell lines. (A) Western blot images of PI3K/AKT/GSK-3β signaling pathway-related proteins in UT, PTEN-WT and PTEN-KO cells. (B) Immunocytochemistry analysis targeting β-catenin (1000×). (C) Western blot images of EMT signaling pathway-related proteins in UT, PTEN-WT and PTEN-KO cells. (D Immunocytochemistry analysis targeting E-Cadherin (1000X). (E&F) Immunocytochemistry analysis targeting N-Cadherin and vimentin (1000X). (G) The morphologies of PTEN-KO cell lines. Cells were photographed by phase-contrast microscopy. PTEN-KO cells show morphological changes associated with EMT: presence of round shape cells, spindle-shape and loss of cell-cell interaction (upper panels). In the colony formation assay, the colony shape of PTEN-KO cells became fuzzy in both cells compared with PTEN-WT cells. Each experiment was triplicated. β-catenin (green); E-Cadherin (green); N-Cadherin (red); vimentin (green); nuclei (Lamin-B1, red) or (Hoechst 33342, blue).

and upregulated in lung cancer, which is associated with tumor progression [34]. CXCL12 and its receptor CXCR4 are known to be involved in regulation of metastasis and their protein expressions have been shown to be elevated in various types of metastatic cancers including lung, colon, breast cancers [35,36]. Earlier studies reported that PTEN loss mediates migration and invasion of prostate cancer cells through activation of PI3K/AKT signaling in response to CXCL12/CXCR4 [37,38]. Consistent with the previous reports, expressions of CXCR4/CXCL12 and CXCR1/CXCL8 were elevated in PTEN-KO cells in our study.

There are several limitations in this study. KRAS mutation is one of the common mutation events in NSCLC, which occurs in approximately

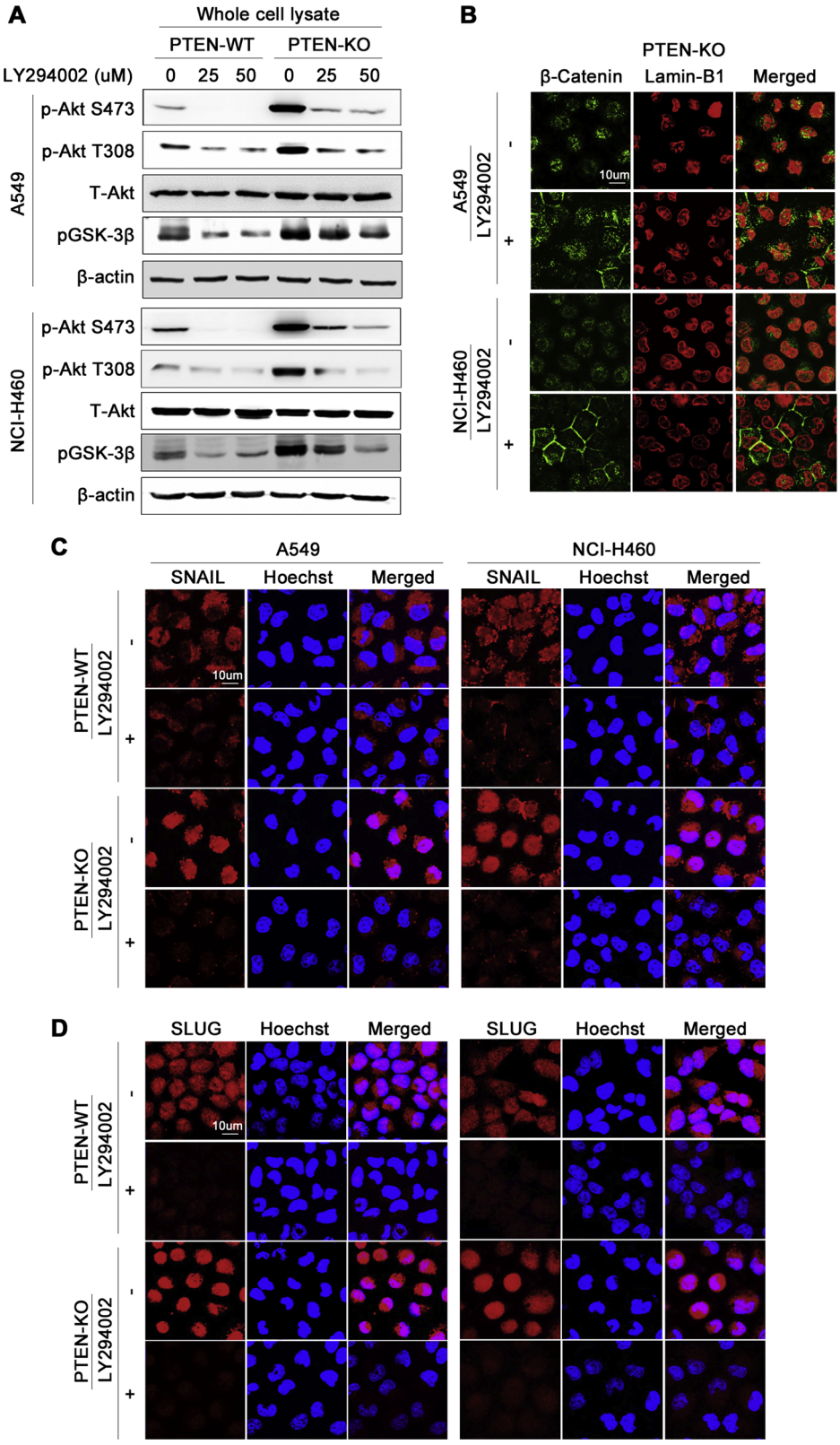

Fig. 5. Localization of β-catenin, Slug and Snail in PI3K inhibitor (LY294002) treated cells. A549 and NCI-H460 cells were treated with 50μM of PI3K inhibitor for 6 h and subjected to immunoblot and immunofluorescence analysis for β-catenin, Slug and Snail. (A) Western blot images of AKT/pGSK-3ß signaling proteins at 6 h time point after treating PTEN-KO and WT cells with LY294002 (0, 25 u M and 50 u M). (B, C & D) Immunocytochemistry analysis targeting β-catenin, Snail, and Slug (1000×). β-catenin (green), Snail (red), Slug (red), and nuclei (blue: Hoechst 33342) or (red: Lamin-B1).

10–15% of NSCLCs in Asia [39]. It has been suggested that PTEN inactivation accelerates KRAS mutation-initiated lung tumorigenesis [40]. In this study, we did not explore the correlation between PTEN inactivation in lung cancer with/without KRAS mutation because both cell lines were KRAS mutants. Secondly, a recent study suggested that addition of a PI3K-mTOR inhibitor attenuated tumor growth when

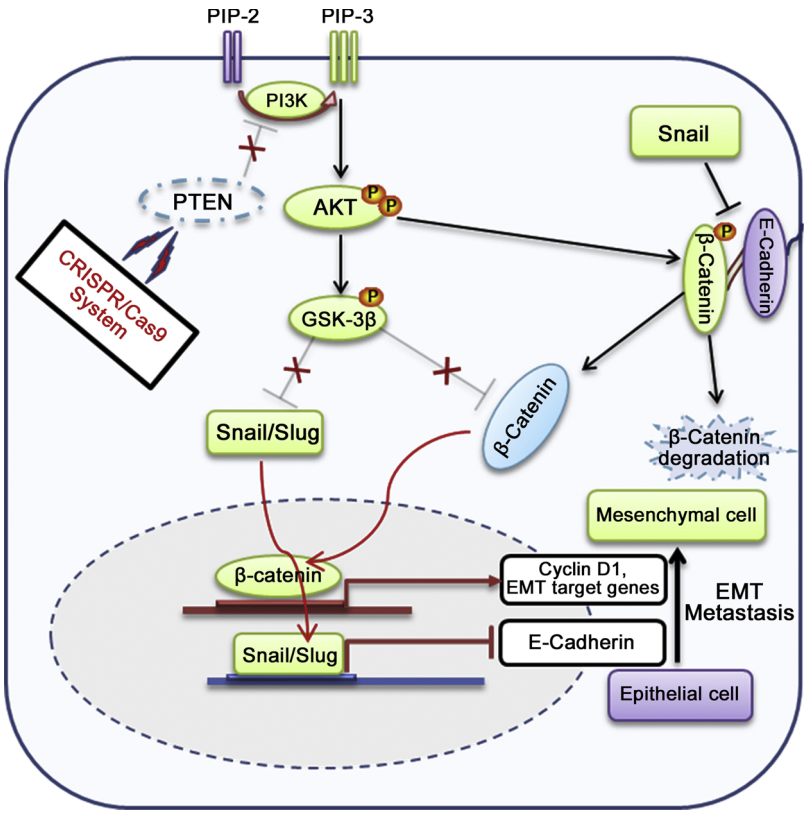

Fig. 6. A proposed model of PI3K/AKT/GSK-3β/β-catenin/Snail signaling mediated EMT in PTEN-KO lung cancer cell lines.

compared with chemotherapy alone in a PTEN deficient PDXs [41], suggesting the therapeutic applicability of PI3K inhibitor. Although LY294002 treatment resulted in downregulation of p-AKT in this study, we did not explore the therapeutic potential of LY294002. Further studies with a large NSCLC group with proper clinical and genetic information will be required to verify this point.

In conclusion, the present study revealed that PTEN inactivation contributes to EMT and metastasis by nuclear translocation of β-catenin and Snail/Slug in lung cancer cells. Through PI3K inhibitor treatment to PTEN-KO cells, we confirmed that the PI3K/AKT/GSK-3β pathway was essential for inducing EMT in PTEN inactivated cells. Our data provide a better understanding of detailed molecular mechanism of metastasis related with inactivation of PTEN, which can help to understand distant metastasis in lung cancer.

Conflicts of interest

The authors declare no conflict of interest

Acknowledgments

This study was supported by a grant from National Research Foundation of Korea (2017R1E1A1A01074913, 2012R1A5A2047939, 2012R1A1A3002027 and 2017M3C9A6047615).

Appendix A. Supplementary data

Supplementary material related to this article can be found, in the online version, at doi:https://doi.org/10.1016/j.lungcan.2019.01.013.

References

[1] J.R. Molina, P. Yang, S.D. Cassivi, S.E. Schild, A.A. Adjei, Non-small cell lung cancer: epidemiology, risk factors, treatment, and survivorship, Mayo Clin. Proc. 83 (5) (2008) 584–594.
[2] F.L.M. Ervik, J. Ferlay, L. Mery, I. Soerjomataram, F. Bray, Cancer Today, International Agency for Research on Cancer, Lyon, France, 2016http://gco.iarc.fr/today/home.
[3] W.A. Castrucci, J.P. Knisely, An update on the treatment of CNS metastases in small cell lung cancer, Cancer J. 14 (3) (2008) 138–146.
[4] G.R. Mundy, Metastasis to bone: causes, consequences and therapeutic opportunities, Nat. Rev. Cancer 2 (8) (2002) 584–593.
[5] D. Kong, Y. Li, Z. Wang, F.H. Sarkar, Cancer stem cells and epithelial-to-mesenchymal transition (EMT)-phenotypic cells: are they cousins or twins? Cancers (Basel) 3 (1) (2011) 716–729.
[6] G. Wang, W. Dong, H. Shen, X. Mu, Z. Li, X. Lin, Y. Liu, J. Du, A comparison of Twist and E-cadherin protein expression in primary non-small-cell lung carcinoma and corresponding metastases, Eur. J. Cardiothorac. Surg. 39 (6) (2011) 1028–1032.
[7] M.S. Song, L. Salmena, P.P. Pandolfi, The functions and regulation of the PTEN tumour suppressor, Nat. Rev. Mol. Cell Biol. 13 (5) (2012) 283–296.
[8] L. Bao, Y. Yan, C. Xu, W. Ji, S. Shen, G. Xu, Y. Zeng, B. Sun, H. Qian, L. Chen, M. Wu, C. Su, J. Chen, MicroRNA-21 suppresses PTEN and hSulf-1 expression and promotes hepatocellular carcinoma progression through AKT/ERK pathways, Cancer Lett. 337 (2) (2013) 226–236.
[9] F. Vazquez, W.R. Sellers, The PTEN tumor suppressor protein: an antagonist of phosphoinositide 3-kinase signaling, Biochim. Biophys. Acta 1470 (1) (2000) M21–35.
[10] A. Di Cristofano, P.P. Pandolfi, The multiple roles of PTEN in tumor suppression, Cell 100 (4) (2000) 387–390.
[11] E. Rhei, L. Kang, F. Bogomolniy, M.G. Federici, P.I. Borgen, J. Boyd, Mutation analysis of the putative tumor suppressor gene PTEN/MMAC1 in primary breast carcinomas, Cancer Res. 57 (17) (1997) 3657–3659.
[12] A. Sobczuk, B. Smolarz, H. Romanowicz-Makowska, T. Pertynski, MMAC/PTEN gene expression in endometrial cancer: RT-PCR studies, Pol. J. Pathol. 57 (3) (2006) 137–140.
[13] Y. Zhao, R. Zheng, J. Li, F. Lin, L. Liu, Loss of phosphatase and tensin homolog expression correlates with clinicopathological features of non-small cell lung cancer patients and its impact on survival: a systematic review and meta-analysis, Thorac. Cancer 8 (3) (2017) 203–213.
[14] J.C. Soria, H.Y. Lee, J.I. Lee, L. Wang, J.P. Issa, B.L. Kemp, D.D. Liu, J.M. Kurie, L. Mao, F.R. Khuri, Lack of PTEN expression in non-small cell lung cancer could be related to promoter methylation, Clin. Cancer Res. 8 (5) (2002) 1178–1184.
[15] C.J. Marsit, S. Zheng, K. Aldape, P.W. Hinds, H.H. Nelson, J.K. Wiencke, K.T. Kelsey, PTEN expression in non-small-cell lung cancer: evaluating its relation to tumor characteristics, allelic loss, and epigenetic alteration, Hum. Pathol. 36 (7) (2005) 768–776.
[16] J.M. Tang, Q.Y. He, R.X. Guo, X.J. Chang, Phosphorylated Akt overexpression and loss of PTEN expression in non-small cell lung cancer confers poor prognosis, Lung

Cancer 51 (2) (2006) 181–191.
[17] T. Kohnoh, N. Hashimoto, A. Ando, K. Sakamoto, S. Miyazaki, D. Aoyama, M. Kusunose, M. Kimura, N. Omote, K. Imaizumi, T. Kawabe, Y. Hasegawa, Hypoxia-induced modulation of PTEN activity and EMT phenotypes in lung cancers, Cancer Cell Int. 16 (2016) 33.
[18] D. Aoyama, N. Hashimoto, K. Sakamoto, T. Kohnoh, M. Kusunose, M. Kimura, R. Ogata, K. Imaizumi, T. Kawabe, Y. Hasegawa, Involvement of TGFbeta-induced phosphorylation of the PTEN C-terminus on TGFbeta-induced acquisition of malignant phenotypes in lung cancer cells, PLoS One 8 (11) (2013) e81133.
[19] T.D. Schmittgen, K.J. Livak, Analyzing real-time PCR data by the comparative C(T) method, Nat. Protoc. 3 (6) (2008) 1101–1108.
[20] J. Li, Z. Deng, Z. Wang, D. Wang, L. Zhang, Q. Su, Y. Lai, B. Li, Z. Luo, X. Chen, Y. Chen, X. Huang, J. Ma, W. Wang, J. Bi, X. Guan, Zipper-interacting protein kinase promotes epithelial-mesenchymal transition, invasion and metastasis through AKT and NF-kB signaling and is associated with metastasis and poor prognosis in gastric cancer patients, Oncotarget 6 (10) (2015) 8323–8338.
[21] N. Yanagawa, C. Leduc, D. Kohler, M.A. Saieg, T. John, J. Sykes, M. Yoshimoto, M. Pintilie, J. Squire, F.A. Shepherd, M.S. Tsao, Loss of phosphatase and tensin homolog protein expression is an independent poor prognostic marker in lung adenocarcinoma, J. Thorac. Oncol. 7 (10) (2012) 1513–1521.
[22] D. Fang, D. Hawke, Y. Zheng, Y. Xia, J. Meisenhelder, H. Nika, G.B. Mills, R. Kobayashi, T. Hunter, Z. Lu, Phosphorylation of beta-catenin by AKT promotes beta-catenin transcriptional activity, J. Biol. Chem. 282 (15) (2007) 11221–11229.
[23] H. Wang, H.S. Wang, B.H. Zhou, C.L. Li, F. Zhang, X.F. Wang, G. Zhang, X.Z. Bu, S.H. Cai, J. Du, Epithelial-mesenchymal transition (EMT) induced by TNF-alpha requires AKT/GSK-3beta-mediated stabilization of snail in colorectal cancer, PLoS One 8 (2) (2013) e56664.
[24] Z.C. Liu, H.S. Wang, G. Zhang, H. Liu, X.H. Chen, F. Zhang, D.Y. Chen, S.H. Cai, J. Du, AKT/GSK-3beta regulates stability and transcription of snail which is crucial for bFGF-induced epithelial-mesenchymal transition of prostate cancer cells, Biochim. Biophys. Acta 1840 (10) (2014) 3096–3105.
[25] A. Cavazzoni, S. La Monica, R. Alfieri, A. Ravelli, N. Van Der Steen, R. Sciarrillo, D. Madeddu, C.A.M. Lagrasta, F. Quaini, M. Bonelli, C. Fumarola, D. Cretella, G. Digiacomo, M. Tiseo, G.J. Peters, A. Ardizzoni, P.G. Petronini, E. Giovannetti, Enhanced efficacy of AKT and FAK kinase combined inhibition in squamous cell lung carcinomas with stable reduction in PTEN, Oncotarget 8 (32) (2017) 53068–53083.
[26] C. Lu, Z. Shan, J. Hong, L. Yang, MicroRNA-92a promotes epithelial-mesenchymal transition through activation of PTEN/PI3K/AKT signaling pathway in non-small cell lung cancer metastasis, Int. J. Oncol. 51 (1) (2017) 235–244.
[27] M.C. Boelens, M. Nethe, S. Klarenbeek, J.R. de Ruiter, E. Schut, N. Bonzanni, A.L. Zeeman, E. Wientjens, E. van der Burg, L. Wessels, R. van Amerongen, J. Jonkers, PTEN loss in E-cadherin-deficient mouse mammary epithelial cells rescues apoptosis and results in development of classical invasive lobular carcinoma, Cell Rep. 16 (8) (2016) 2087–2101.
[28] J.H. Cho, J.P. Robinson, R.A. Arave, W.J. Burnett, D.A. Kircher, G. Chen, M.A. Davies, A.H. Grossmann, M.W. VanBrocklin, M. McMahon, S.L. Holmen, AKT1 activation promotes development of melanoma metastases, Cell Rep. 13 (5) (2015) 898–905.
[29] J.K. Rho, Y.J. Choi, J.K. Lee, B.Y. Ryoo, I.I. Na, S.H. Yang, C.H. Kim, J.C. Lee, Epithelial to mesenchymal transition derived from repeated exposure to gefitinib determines the sensitivity to EGFR inhibitors in A549, a non-small cell lung cancer cell line, Lung Cancer 63 (2) (2009) 219–226.
[30] S.C. Wang, X.L. Lin, H.Y. Wang, Y.J. Qin, L. Chen, J. Li, J.S. Jia, H.F. Shen, S. Yang, R.Y. Xie, F. Wei, F. Gao, X.X. Rong, J. Yang, W.T. Zhao, T.T. Zhang, J.W. Shi, K.T. Yao, W.R. Luo, Y. Sun, D. Xiao, Hes1 triggers epithelial-mesenchymal transition (EMT)-like cellular marker alterations and promotes invasion and metastasis of nasopharyngeal carcinoma by activating the PTEN/AKT pathway, Oncotarget 6 (34) (2015) 36713–36730.
[31] B.P. Zhou, J. Deng, W. Xia, J. Xu, Y.M. Li, M. Gunduz, M.C. Hung, Dual regulation of snail by GSK-3beta-mediated phosphorylation in control of epithelial-mesenchymal transition, Nat. Cell Biol. 6 (10) (2004) 931–940.
[32] S. Persad, A.A. Troussard, T.R. McPhee, D.J. Mulholland, S. Dedhar, Tumor suppressor PTEN inhibits nuclear accumulation of beta-catenin and T cell/lymphoid enhancer factor 1-mediated transcriptional activation, J. Cell Biol. 153 (6) (2001) 1161–1174.
[33] A. Cano, M.A. Perez-Moreno, I. Rodrigo, A. Locascio, M.J. Blanco, M.G. del Barrio, F. Portillo, M.A. Nieto, The transcription factor snail controls epithelial-mesenchymal transitions by repressing E-cadherin expression, Nat. Cell Biol. 2 (2) (2000) 76–83.
[34] D.A. Arenberg, S.L. Kunkel, P.J. Polverini, M. Glass, M.D. Burdick, R.M. Strieter, Inhibition of interleukin-8 reduces tumorigenesis of human non-small cell lung cancer in SCID mice, J. Clin. Invest. 97 (12) (1996) 2792–2802.
[35] B. Furusato, A. Mohamed, M. Uhlen, J.S. Rhim, CXCR4 and cancer, Pathol. Int. 60 (7) (2010) 497–505.
[36] F. Guo, Y. Wang, J. Liu, S.C. Mok, F. Xue, W. Zhang, CXCL12/CXCR4: a symbiotic bridge linking cancer cells and their stromal neighbors in oncogenic communication networks, Oncogene 35 (7) (2016) 816–826.
[37] S.R. Chinni, S. Sivalogan, Z. Dong, J.C. Filho, X. Deng, R.D. Bonfil, M.L. Cher, CXCL12/CXCR4 signaling activates Akt-1 and MMP-9 expression in prostate cancer cells: the role of bone microenvironment-associated CXCL12, Prostate 66 (1) (2006) 32–48.
[38] M.A. Chetram, V. Odero-Marah, C.V. Hinton, Loss of PTEN permits CXCR4-mediated tumorigenesis through ERK1/2 in prostate cancer cells, Mol. Cancer Res. 9 (1) (2011) 90–102.
[39] I. Ferrer, J. Zugazagoitia, S. Herbertz, W. John, L. Paz-Ares, G. Schmid-Bindert, KRAS-mutant non-small cell lung cancer: from biology to therapy, Lung Cancer 124 (2018) 53–64.
[40] K. Iwanaga, Y. Yang, M.G. Raso, L. Ma, A.E. Hanna, N. Thilaganathan, S. Moghaddam, C.M. Evans, H. Li, W.W. Cai, M. Sato, J.D. Minna, H. Wu, C.J. Creighton, F.J. Demayo, I.I. Wistuba, J.M. Kurie, Pten inactivation accelerates oncogenic K-ras-initiated tumorigenesis in a mouse model of lung cancer, Cancer Res. 68 (4) (2008) 1119–1127.
[41] I. Brana, N.A. Pham, L. Kim, S. Sakashita, M. Li, C. Ng, Y. Wang, P. Loparco, R. Sierra, L. Wang, B.A. Clarke, B.G. Neel, L.L. Siu, M.S. Tsao, Novel combinations of PI3K-mTOR inhibitors with dacomitinib or chemotherapy in PTEN-deficient patient-derived tumor xenografts, Oncotarget 8 (49) (2017) 84659–84670.